Ning, S. F. Venable, O. M. Pereira-Smith, J. R. Smith, *Exp. Cell Res.* **211**, 90 (1994).
4. Y. Xiong *et al.*, *Nature* **366**, 701 (1993).
5. W. S. El-Deiry *et al.*, *Cell* **75**, 817 (1993); Y. Li, C. W. Jenkins, M. A. Nichols, Y. Xiong, *Oncogene* **9**, 2261 (1994).
6. W. S. El-Deiry *et al.*, *Cancer Res.* **54**, 1169 (1994); A. Di Leonardo, S. P. Linke, K. Clarkin, G. M. Wahl, *Genes Dev.* **8**, 2540 (1994); V. Dulic *et al.*, *Cell* **76**, 1013 (1994).
7. H. Jiang *et al.*, *Oncogene* **9**, 3397 (1994); R. A. Steinman *et al.*, *ibid.*, p. 3389.
8. P. Michieli *et al.*, *Cancer Res.* **54**, 3391 (1994).
9. R. Sen and D. Baltimore, *Cell* **47**, 921 (1986); C. Thevenin *et al.*, *New Biol.* **2**, 793 (1990); A. S. Baldwin, J. C. Azizkhan, D. E. Jensen, A. A. Beg, L. R. Coodly, *Mol. Cell. Biol.* **11**, 4943 (1991); Y. Devary, C. Rosette, J. A. DiDonato, M. Karin, *Science* **261**, 1442 (1993).
10. G. P. Nolan and D. Baltimore, *Curr. Opin. Genet. Dev.* **2**, 211 (1992); M. Grilli, J. J. Chiu, M. J. Lenardo, *Int. Rev. Cytol.* **143**, 1 (1993); U. Siebenlist, G. Franzoso, K. Brown, *Annu. Rev. Cell Biol.* **10**, 405 (1994).
11. G. E. Griffin, K. Leung, T. M. Folks, S. Kunkel, G. J. Nabel, *Nature* **339**, 70 (1989).
12. S. L. Eck, N. D. Perkins, D. P. Carr, G. J. Nabel, *Mol. Cell. Biol.* **13**, 6530 (1993).
13. G. Nabel and D. Baltimore, *Nature* **326**, 711 (1987).
14. C. S. Duckett *et al.*, *Mol. Cell. Biol.* **13**, 1315 (1993).
15. M. Serrano, G. J. Hannon, D. Beach, *Nature* **366**, 704 (1993).
16. G. J. Hannon and D. Beach, *ibid.* **371**, 257 (1994); T. Suzuki, S. Kitao, H. Matsushime, M. Yoshida, *EMBO J.* **15**, 1607 (1996).
17. N. D. Perkins, L. K. Felzien, G. J. Nabel, unpublished data.
18. K. Leung and G. J. Nabel, *Nature* **333**, 776 (1988).
19. L. Osborn, S. Kunkel, G. J. Nabel, *Proc. Natl. Acad. Sci. U.S.A.* **86**, 2336 (1989).
20. W. Lin and L. A. Culp, *Biotechniques* **11**, 344 (1991); N. D. Perkins, A. B. Agranoff, C. S. Duckett, G. J. Nabel, *J. Virol.* **68**, 6820 (1994).
21. Nuclear protein extracts (~125 μg) were incubated at 4°C for 2 hours with anti-RelA (2 μg) (sc-109X; Santa Cruz Biotechnology, Santa Cruz, CA) or control rabbit immunoglobulin G (IgG) in Dignam D buffer [J. D. Dignam, R. M. Lebovitz, R. G. Roeder, *Nucleic Acids Res.* **11**, 1475 (1983)] containing 0.1% NP-40 (adjusted to a final NaCl concentration of 75 mM). Antibody-protein complexes were recovered by incubation for 1 hour with protein G–agarose (10 μl) and low-speed centrifugation. Sedimental material was washed three times with 0.5 ml of incubation buffer [20 mM Hepes (pH 7.9), 75 mM KCl, 2.5 mM $MgCl_2$, 1 mM dithiothreitol (DTT), 0.1% NP-40, 0.5 mM phenylmethylsulfonyl fluoride (PMSF), aprotinin (1 μg/ml), pepstatin A (1 μg/ml), leupeptin (2 μg/ml), and 1 mM sodium vanadate]. For histone H1 kinase assays, protein G–bound complexes were resuspended in 50 μl of kinase buffer [50 mM tris (pH 7.5), 10 mM $MgCl_2$, 1 mM DTT, and 0.5 mM PMSF]. Purified glutathione-S-transferase fusion protein GST-p21 (~50 ng) or GST proteins eluted into kinase buffer containing 10 mM glutathione were added as indicated. The samples were incubated with 133 μCi of [γ-^{32}P]adenosine triphosphate (ATP) and 2 μg of purified histone H1 (Boehringer Mannheim) at 37°C for 15 min with frequent agitation. The reaction was terminated by the addition of SDS gel loading buffer, and a sample was resolved on an SDS-polyacrylamide (15%) gel, which was then dried and subjected to autoradiography. Cyclin-Cdk immunoprecipitations were done as described above for RelA, using 100 or 600 μg of nuclear extract and 10 μg of agarose-conjugated antibodies from Santa Cruz [sc-163AC (Cdk2), sc-601AC (Cdk4), sc-054AC (Cdc2), sc-239AC (cyclin A), sc-245AC (cyclin B1), sc-246AC (cyclin D1), and sc-248AC (cyclin E)]. All antibodies to cyclins were mouse monoclonals (IgG1), the antibodies to Cdk2 and Cdk4 were rabbit polyclonal antibodies to Cdk peptides, and the antibody to Cdc2 was a mouse monoclonal (IgG2a). Protein immunoblotting of RelA was done with a rabbit polyclonal antibody (sc-109, Santa Cruz).
22. S. van den Heuvel and E. Harlow, *Science* **262**, 2050 (1993).
23. Z. Arany, W. R. Sellers, D. M. Livingston, R. Eckner, *Cell* **77**, 799 (1994).
24. Immunoprecipitations and transfections of 293 cells were done as described (Figs. 1 and 2) with antibodies from Pharmingen (14991A for p300 in Fig. 3, A, B, and D) or Santa Cruz [sc-109 (RelA), sc-369 (CBP), and sc-584 (p300 in Fig. 3C)]. Proteins were eluted from RelA (Fig. 3B) by incubation at room temperature for 15 min in wash buffer (*19*) that contained 300 mM KCl and bovine serum albumin (1 mg/ml). Either purified rabbit IgG or mouse IgG2b was used as the control where appropriate. In Fig. 3D, the p300 protein was immunoprecipitated from 200 μg of Jurkat nuclear extract and incubated with the indicated in vitro translated ^{35}S-labeled proteins (TNT rabbit coupled reticulocyte lysate system, Promega). Purified mouse IgG2b was used as the control. Protein association experiments, Bluescript RelA, RelA/VP16, Sp1, NF-κB1(p50), and pET RelA(1–306) plasmids used for in vitro transcription-translation have been described [N. D. Perkins, A. B. Agranoff, E. Pascal, G. J. Nabel, *Mol. Cell. Biol.* **14**, 6570 (1994)].
25. J. R. Lundblad, R. P. S. Kwok, M. E. Laurance, M. L. Harter, R. H. Goodman, *Nature* **374**, 85 (1995); A. J. Bannister and T. Kouzarides, *EMBO J.* **14**, 4758 (1995); R. Janknect and A. Nordheim, *Oncogene* **12**, 1961 (1996); P. Dai *et al.*, *Genes Dev.* **10**, 528 (1996).
26. P. Yaciuk and E. Moran, *Mol. Cell. Biol.* **11**, 5389 (1991); S. E. Abraham, S. Lobo, P. Yaciuk, H. H. Wang, E. Moran, *Oncogene* **8**, 1639 (1993); R. Eckner *et al.*, *Genes Dev.* **8**, 869 (1994); A. C. Banerjee *et al.*, *Oncogene* **9**, 1733 (1994); C. Missero *et al.*, *Proc. Natl. Acad. Sci. U.S.A.* **92**, 5451 (1995).
27. A. M. Ventura, M. Q. Arens, A. Srinivasan, G. Chinnadurai, *Proc. Natl. Acad. Sci. U.S.A.* **87**, 1310 (1990); H. G. Wang *et al.*, *J. Virol.* **67**, 476 (1993); C. Song, P. M. Loewenstein, M. Green, *ibid.* **69**, 2907 (1995); S. F. Parker, L. K. Felzien, N. D. Perkins, M. J. Imperiale, G. J. Nabel, *J. Virol.*, in press.
28. R. Roy *et al.*, *Cell* **79**, 1093 (1994); R. Shiekhattar *et al.*, *Nature* **374**, 283 (1995); S.-M. Liao *et al.*, *ibid.*, p. 193; H.-P. Gerber *et al.*, *ibid.*, p. 660.
29. T. D. Gilmore and H. M. Temin, *Cell* **44**, 791 (1986); A. Neri *et al.*, *ibid.* **67**, 1075 (1991).
30. F. Petrij *et al.*, *Nature* **376**, 348 (1995); M. Muraoka *et al.*, *Oncogene* **12**, 1565 (1996).
31. J. He *et al.*, *J. Virol.* **69**, 6705 (1995); J. B. M. Jowett *et al.*, *ibid.*, p. 6304; S. R. Bartz, M. E. Rogel, M. Emerman, *ibid.* **70**, 2324 (1996).
32. The antibodies to p300 used were 14991A (Pharmingen) and sc-584 (Santa Cruz); the antibodies to CBP, TBP, $TAF_{II}250$, $TAF_{II}130$, TFIIH p89 subunit, Cdk2, cyclin A, cyclin B1, and cyclin E were from Santa Cruz (sc-369, sc-204, sc-735, sc-736, sc-293, sc-163, sc-239AC, sc-245AC, and sc-248AC, respectively). The p300 cDNAs were obtained by polymerase chain reaction (PCR) amplified with the EXPAND PCR kit (Boehringer) from polyadenylated RNA (0.5 μg) from human spleen (Clontech) with oligo(dT) as a primer and reverse transcriptase (Stratagene). A 5′ fragment (sense, 5′-GCTAAGCTTCACCATGGCCGAGAATG-TGGTGGAACCGGGGCCG-3′; antisense, 5′-CACA-GATCTGATGCATCTTTCTTCCGCACTCTGTAC-3′), as well as a 3′ p300 fragment overlapping the internal Bgl II site (sense, 5′-ATCAGATCTGTGTCCT-TCACCATGAGATCATCTGGC-3′; antisense, 5′-GC-TAGATCTCTAGTGTATGTCTAGTGTACTCTGTG-AGAGG-3′) were isolated and subcloned into pBluescript downstream of the T7 promoter.
33. We thank D. Gschwend for secretarial assistance; N. Barrett and K. Carter for preparation of figures; G. Hannon for p21 and p16 plasmids; P. Hobart (Vical Inc.) for the VCL-1012 CMV expression plasmid; G. Enders, J. LaBaer, and E. Harlow for the dominant negative Cdk2 plasmid; and W. Kong, Z. Yang, S. Parker, and other members of the Nabel lab for their advice and comments. N.D.P. is the recipient of a Scholar Award from the American Foundation for AIDS Research (AmFAR) in memory of James Hoese. Supported in part by NIH grant RO1 AI29179.

15 July 1996; accepted 25 November 1996

A Legume Ethylene-Insensitive Mutant Hyperinfected by Its Rhizobial Symbiont

R. Varma Penmetsa and Douglas R. Cook*

Development of the *Rhizobium*-legume symbiosis is controlled by the host plant, although the underlying mechanisms have remained obscure. A mutant in the annual legume *Medicago truncatula* exhibits an increase of more than an order of magnitude in the number of persistent rhizobial infections. Physiological and genetic analyses indicate that this same mutation confers insensitivity to the plant hormone ethylene for multiple aspects of plant development, including nodulation. These data support the hypothesis that ethylene is a component of the signaling pathway controlling rhizobial infection of legumes.

In contrast to pathogenic plant-microbe interactions where persistent infection is correlated with cellular dysfunction and disease, compatible rhizobia trigger morphogenesis of a nodule organ and symbiotic nitrogen fixation on their legume host plant. Despite the beneficial aspects of this symbiosis, rhizobial infection is regulated by the plant host. One mechanism for controlling infection by compatible rhizobia, referred to as feedback inhibition of nodulation, is evidenced as a transient susceptibility to rhizobial infection in root hair cells (*1*). This transient susceptibility results in a narrow zone of infection and nodule differentiation (Fig. 1A). Plant mutants defective in feedback inhibition of nodulation continue to produce nodules from newly developed root tissue (*2*). A possible second mechanism for controlling rhizobial infection involves the early arrest of rhizobial infections within the nodulation zone; in fact, only a minority of rhizobial infections

Department of Plant Pathology and Microbiology, Crop Biotechnology Center, and Graduate Program in Genetics, Texas A&M University, College Station, TX 77843, USA.

*To whom correspondence should be addressed.

persist to colonize differentiating nodule tissue. Vasse *et al.* (*3*) observed that many such infections arrest after infection structures (infection threads) penetrate one to several cells, and plant cells containing arrested infections often display characteristics of induced host defense mechanisms (*3*, *4*).

A possible clue to the physiology underlying rhizobial infection arrest comes from the observation that inhibitors of ethylene biosynthesis, such as aminoethoxyvinyl glycine (AVG), cause an increase in persistent rhizobial infections (*5*, *6*). Certain rhizobia produce rhizobitoxine, an analog of AVG, although roles in nodulation or regulation of ethylene synthesis in plants have not been demonstrated (*7*). Conversely, application of ethylene reduces nodulation in wild-type pea (*8*), and ethylene has been implicated as a second signal in the inhibition of nodulation by both light and nitrate (*9*). Thus, ethylene may provide an endogenous signal for regulation of rhizobial infection, and plant mutants with defects in production or transduction of the ethylene signal might be expected to have correspondingly altered infection phenotypes.

We screened a population of ethylmethane sulfonate (EMS)–mutagenized seedlings of *M. truncatula* for defects in symbiotic interactions. Using a visual assay for nodulation, we identified putative symbiotic mutants, including non-nodulators and those with altered nodule development (*10*). To determine whether any of these mutants were defective in rhizobial infection, we transformed the bacterial symbiont *Rhizobium meliloti* with a constitutively expressed *lacZ* gene (*11*). This modified strain converts the colorless X-Gal substrate to an insoluble blue precipitate and thus provides a visual assay for rhizobial infection (*12*). Initially we characterized infection in wild-type *M. truncatula*. We determined that initiation of infection was complete by 48 hours, resulting in 100 to 300 visible infections within the nodulation zone (Fig. 1E). At 72 hours, an average of eight macroscopic nodule primordia were evident, each of which were associated with extensive rhizobial infection (Fig. 1D) and subsequently developed into mature nitrogen-fixing nodules. Infection events not associated with nodule morphogenesis were typically arrested in the root epidermis (Fig. 1, B and C). Thus, the infection efficiency of wild-type *M. truncatula* is low, with 3 to 8% of the infections persisting to colonize a nodule organ.

We used this modified *Rhizobium* strain to assess infection in the M_3 and F_2 backcross generations of previously identified nodulation mutants. One such mutant, named *sickle* for its unusual sickle-shaped zone of nodulation (Fig. 2A), contained an increase of more than an order of magnitude in the number of sustained infections relative to the wild type (Fig. 2, B and C). The *sickle* mutation affects the number of persistent infections without altering the transience of root susceptibility (Fig. 2A); thus, the corresponding gene is implicated in arrest of rhizobial infection within the nodulation zone, but not in feedback inhibition of nodulation. Sustained infections in *sickle* were characterized by infection threads that ramified into the root cortex toward developing nodule primordia (Fig. 2D), similar to sustained infection in wild-type plants. Cytological, physiological, and molecular analyses (Fig. 2, E and F, Table 1, and Fig. 3) revealed apparently normal differentiation of both symbionts, although nodule morphogenesis in *sickle* was retarded relative to the wild type (*13*).

In a manner consistent with a defect in ethylene production or perception (*14*, *15*), *sickle* plants were pleiotropic for delayed

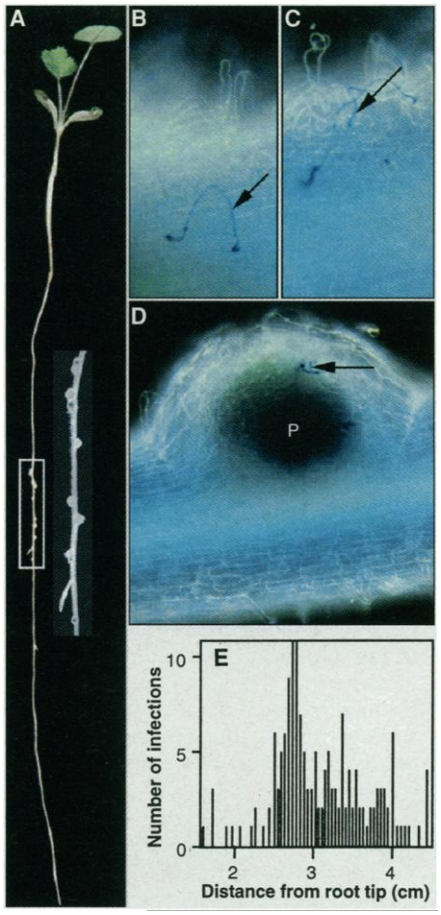

Fig. 1. Distribution of *R. meliloti* infections and nodules on *M. truncatula* roots. (**A**) Nodulation zone on roots 10 days after inoculation with *R. meliloti*. The inset shows an expanded view of the nodulation zone. (**B** to **D**) Arrested [(B) and (C)] and successful (D) infections, respectively, within the nodulation zone 120 hours after inoculation with *R. meliloti*. Blue coloration identifies bacteria expressing the *lacZ* gene within infected root hair cells (arrow). In (D), P denotes a nodule primordium colonized by bacteria from a single infection event (arrow). (**E**) Distribution of *lacZ*-stained infections 48 hours after inoculation with *R. meliloti*.

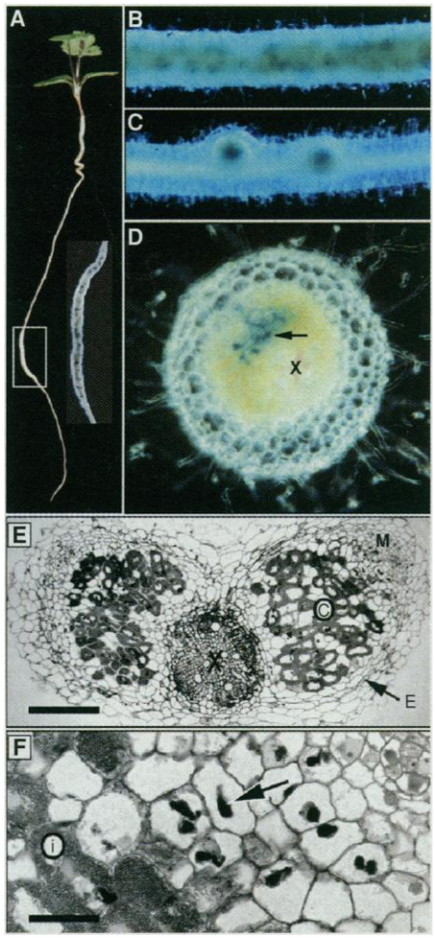

Fig. 2. Infection and nodulation phenotype of the *M. truncatula* mutant *sickle*. (**A**) Nodulation zone on *sickle* roots 10 days after inoculation with *R. meliloti*. Note that the zone of infection and morphogenesis in *sickle* (inset) is confined to a narrow region, similar to the wild type (Fig. 1A). (**B** and **C**) Nodulation zone on *sickle* and wild-type plants, respectively, 96 hours after inoculation. Persistent infections are visible as blue-staining regions. (**D**) Hand section through a 96-hour infection on a *sickle* root comparable to that shown in (B). The branched infection thread (arrow) has ramified into the root inner cortex. X, xylem tissue in the root vasculature. (**E**) Bright-field micrograph showing tissue differentiation typical of 21-day-old *sickle* nodules. X, root xylem tissue; C, nodule central tissue; E, nodule endodermis; M, nodule meristem. (**F**) Enlargement of (E) showing a gradient of cell differentiation from the infection zone through the adjacent nitrogen fixation zone. The arrow indicates an infection thread in a cell of the infection zone; "i" identifies an infected cell within the nitrogen fixation zone. Scale bars: 20 μm (E) and 120 μm (F).

petal (Fig. 4, A and B) and leaf senescence and for decreased abscission of seed pod and leaves. We assayed the sensitivity of wild-type and *sickle* seedlings to 1-aminocyclopropane carboxylic acid (ACC), the immediate precursor of ethylene, and to ethylene gas. Both ACC and ethylene induced the "triple response" (*14–16*) in wild-type seedlings, including inhibition of root and hypocotyl elongation and formation of a hypocotyl hook (Fig. 4C), whereas *sickle* seedlings were insensitive to both compounds even at >10 times their median effective dose (ED_{50}) values in the wild type (Fig. 4, D and E). Taken together, the ethylene and ACC results indicate that *sickle*, like mutants in *Arabidopsis* and tomato (*14, 17–19*), is defective in perception of the ethylene signal.

To determine the sensitivity of nodulation in wild-type and *sickle* plants to ACC, we grew seedlings in growth pouches and added ACC directly to the growth medium at various times after inoculation with *Rhizobium*. When ACC was added 24 to 48 hours after inoculation, nodulation of wild-type plants was effectively blocked ($ED_{50} \leq 5$ μM; Fig. 5A). Similar treatment of *sickle* failed to inhibit nodulation even at 300 μM ACC (Fig. 5, B to E). After macroscopic nodule primordia were evident (72 hours), continued nodule development on the wild type was largely insensitive to exogenous ACC (Fig. 5A).

Genetic analysis indicates that the hyperinfectable and ethylene-insensitive phenotypes of *sickle* are determined by a single, recessive allele. We assayed cosegregation of hyperinfectability and ethylene-related phenotypes by testing F_2 progeny sequentially for nodulation and ethylene-induced chlorophyll loss (*20*). From a total of 201 F_2 individuals, 50 were hyperinfected and ethylene-insensitive, and 151 were normally infected and ethylene-sensitive ($P = 0.97$, $\chi^2 = 0.0017$). We have designated the corresponding *M. truncatula* gene as *skl1* and the *sickle* allele as *skl1-1*. The pleiotropic nature of *skl1-1* indicates that *skl1* acts in the ethylene perception pathway, similar to mutants in *Arabidopsis*, such as *ein2* and *ein3* (*19*). The recessive nature of *skl1-1* indicates that *skl1* is probably not a member of the ethylene receptor gene family (including *ein1/etr1*), because all known mutants in this family have dominant phenotypes (*17, 18*).

Our results support the hypothesis that ethylene is involved in controlling the persistence of rhizobial infection. Ethylene is

Table 1. Nitrogenase activity in wild-type *M. truncatula* and in the nodulation mutants, *sickle* and *domi*. *domi* is a non-nodulating mutant of *M. truncatula* that is resistant to infection by *Rhizobium* (*10*). Nitrogenase activity was determined by the acetylene reduction assay (*27*), where nitrogenase enzyme reduces substrate acetylene to ethylene. Acetylene reduction was measured on nine roots for each genotype, 19 days after inoculation with *Rhizobium*.

Genotype	Nitrogenase activity (pmol ethylene min^{-1} $root^{-1}$ ± SE)
A17 (wild type)	120 ± 70
sickle (hypernodulating)	220 ± 70
domi (non-nodulating)	0.3 ± 0.3

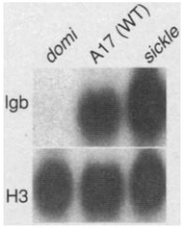

Fig. 3. Leghemoglobin expression in wild-type *M. truncatula* and nodulation mutants. Lanes contain total RNA from roots 23 days after inoculation with *Rhizobium* [lbg, leghemoglobin (*25*); H3, control histone expression (*26*)]. Comparable root tissue was assayed for nitrogenase activity (Table 1) and tissue differentiation (Fig. 2, E and F).

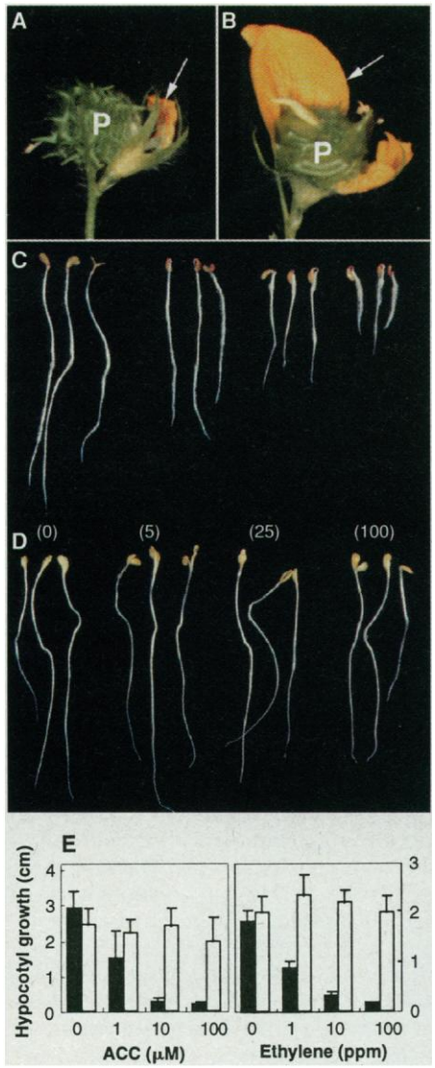

Fig. 4. Ethylene-related phenotypes in wild-type and *sickle* genotypes of *M. truncatula*. (**A** and **B**) Normal and delayed petal senescence (arrows) in the wild type and *sickle*, respectively, 7 days after pollination. P, immature pod. (**C** and **D**) Sensitivity of 5-day-old wild-type (C) and *sickle* (D) seedlings to exogenous ACC (0 to 100 μM, at the values shown in parentheses). The triple response of the wild type to ACC is evidenced by shortened hypocotyls and roots and by hypocotyl hook formation. (**E**) Hypocotyl growth response of wild-type (solid bars) and *sickle* (open bars) seedlings to exogenous ACC and to ethylene gas.

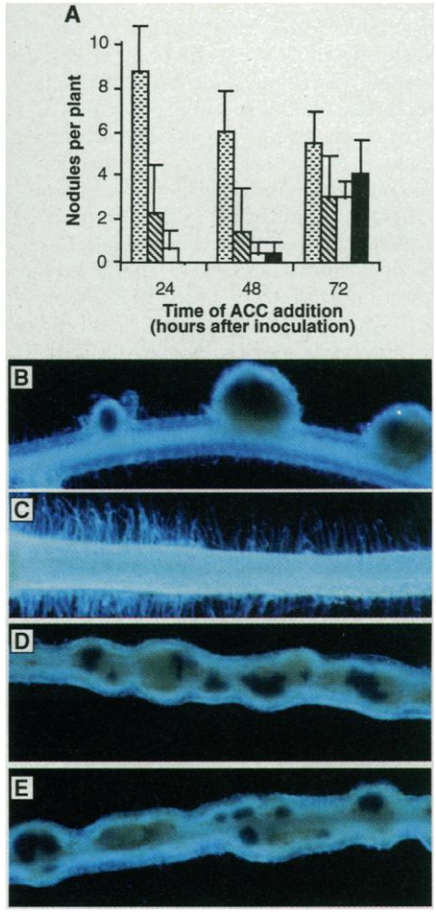

Fig. 5. Effect of ACC on nodulation in wild-type and *sickle* genotypes of *M. truncatula*. (**A**) Suppression of nodulation in the wild type by ACC as a function of symbiotic development. Nodulation is efficiently suppressed when ACC is applied during the primary infection phase (24 and 48 hours), but not when ACC is applied after the appearance of macroscopic nodule primordia (72 hours). Stippled bars, no ACC; hatched bars, 5 μM ACC; open bars, 25 μM ACC; solid bars, 100 μM ACC. (**B** to **E**) Nodulation in the absence (B and D) or presence (C and E) of 300 μM ACC. ACC treatment inhibits nodulation in the wild type (B and C) but not in *sickle* (D and E). Sustained infections are visible as blue-staining tissue.

known to control differentiation of root hair cells (*21*, *22*), the cell type infected by *Rhizobium*. Thus, endogenous ethylene may affect the persistence of rhizobial infection by controlling the formation of infectable root hair cells. Alternatively, ethylene may act as a diffusible signal for activation of mechanisms that arrest rhizobial infection. ACC is inhibitory to nodulation when applied after the initiation of rhizobial infection (Fig. 5A, 24 and 48 hours). Similarly, the ethylene biosynthesis inhibitor AVG can increase nodule number when applied after the initiation of infection (*5*). These observations are consistent with a model wherein endogenous ethylene acts subsequent to infection initiation and root hair differentiation.

If ethylene provides a signal for induction of infection arrest, then plant cells containing persistent *Rhizobium* infections either must avoid the ethylene signal or must be insensitive to the signal. Localized production of ethylene at sites of infection arrest could facilitate avoidance of ethylene by infections destined for nodule colonization. A model for cell-specific regulation of ethylene synthesis during root hair cell differentiation has been proposed in *Arabidopsis* (*22*). In wild-type *M. truncatula*, all rhizobial infections can be blocked by treatment with ACC as late as 48 hours after inoculation (Fig. 5A), indicating that infections destined for nodule colonization are not inherently insensitive to ethylene. However, after macroscopic nodule primordia appear, nodulation is largely insensitive to exogenous ACC (Fig. 5A, 72 hours); thus, sustained rhizobial infections may acquire insensitivity to ethylene.

In plant-pathogen interactions, ethylene has been implicated as an endogenous cue for induction of host defense-related genes (*23*). Despite extensive correlative data, however, a causal role for ethylene in resistance to pathogens has not been established (*24*). In *M. truncatula*, the *sickle* mutation causes extensive developmental abnormalities and hyperinfection by *Rhizobium*, which indicates that *skl1* encodes a function common to both plant development and control of rhizobial infection.

REFERENCES AND NOTES

1. T. Bhuvaneswari, A. A. Bhagwat, W. D. Bauer, *Plant Physiol.* **68**, 1144 (1981); G. Caetano-Anolles and W. D. Bauer, *Planta* **175**, 546 (1988); G. Caetano-Anolles and P. M. Gresshoff, *J. Plant Physiol.* **138**, 765 (1991).
2. B. J. Carroll, D. L. McNeil, P. M. Gresshoff, *Plant Physiol.* **78**, 34 (1985); *Proc. Natl. Acad. Sci. U.S.A.* **82**, 4162 (1985).
3. J. Vasse, F. de Billy, G. Truchet, *Plant J.* **4**, 555 (1993).
4. K. Niehaus, D. Kapp, A. Puhler, *Planta* **190**, 415 (1993); S. Perotto, N. J. Brewin, E. L. Kannenberg, *Mol. Plant-Microbe Interact.* **7**, 99 (1994).
5. N. K. Peters and D. K. Crist-Estes, *Plant Physiol.* **91**, 690 (1989).
6. J. C. Fearn and T. A. LaRue, *ibid.* **96**, 239 (1991); F. C. Guinel and T. A. LaRue, *ibid.* **97**, 1206 (1991); *ibid.* **99**, 515 (1992).
7. X. Ruan and N. K. Peters, *J. Bacteriol.* **174**, 3467 (1992).
8. K. H. Lee and T. A. LaRue, *Plant Physiol.* **100**, 1759 (1992).
9. F. Ligero *et al.*, *ibid.* **97**, 1221 (1991); K. H. Lee and T. A. LaRue, *ibid.* **100**, 1334 (1992).
10. R. V. Penmetsa and D. R. Cook, in preparation.
11. S. A. Leong, P. H. Williams, G. S. Ditta, *Nucleic Acids Res.* **13**, 5965 (1985).
12. C. Boivin *et al.*, *Plant Cell* **2**, 1157 (1990). X-Gal is 5-bromo-4-chloro-3-indolyl-β-D-galactopyranoside.
13. Infections and nodule primordia are first evident on wild-type and *sickle* roots by 36 to 48 hours after inoculation. However, nodule development is retarded in *sickle*, such that 21-day-old nodules are about one-tenth the size of wild-type nodules of similar age.
14. M. B. Lanahan *et al.*, *Plant Cell* **6**, 521 (1994).
15. J. R. Ecker, *Science* **268**, 667 (1995).
16. L. I. Knight, R. C. Rose, W. Crocker, *ibid.* **31**, 635 (1910); P. Guzman and J. R. Ecker, *Plant Cell* **2**, 513 (1990).
17. A. B. Bleecker, M. A. Estelle, C. Somerville, H. Kende, *Science* **241**, 1086 (1988).
18. J. Hua, C. Chang, Q. Sun, E. M. Meyerowitz, *ibid.* **269**, 1712 (1995); C. Chang and E. M. Meyerowitz, *Proc. Natl. Acad. Sci. U.S.A.* **92**, 4129 (1995).
19. G. Roman *et al.*, *Genetics* **139**, 1393 (1995).
20. Isolated leaves were floated on water and treated with ethylene (100 ppm) (*17*). After 5 days dark incubation at 21°C, leaves of wild-type and *sickle* controls were chlorotic and green, respectively.
21. J. D. Masucci and J. W. Schiefelbein, *Plant Cell* **8**, 1505 (1996); *Plant Physiol.* **106**, 1335 (1994).
22. M. Tanimoto, K. Roberts, L. Dolan, *Plant J.* **8**, 943 (1995).
23. J. R. Ecker and R. W. Davis, *Proc. Natl. Acad. Sci. U.S.A.* **84**, 5202 (1987); F. Mauch, J. B. Meehl, A. J. Staehelin, *Planta* **186**, 367 (1992).
24. A. F. Bent *et al.*, *Mol. Plant-Microbe Interact.* **5**, 372 (1992); P. Silverman *et al.*, *ibid.* **6**, 775 (1993); K. Lawton *et al.*, *ibid.* **8**, 863 (1995).
25. F. deBilly *et al.*, *Plant J.* **1**, 27 (1991).
26. N. Chaubet, B. Clement, C. Gigot, *J. Mol. Biol.* **225**, 569 (1992).
27. P. Somasegaran and H. J. Hoben, *Handbook for Rhizobia: Methods in Legume*-Rhizobium *Technology* (Springer-Verlag, New York, 1994), pp. 392–398.

28. Supported by grants from the NSF Program on Integrative Plant Biology (IBN-9507535) and from the Samuel Roberts Noble Foundation.

15 July 1996; accepted 2 December 1996

Measuring Serotonin Distribution in Live Cells with Three-Photon Excitation

S. Maiti, Jason B. Shear,* R. M. Williams, W. R. Zipfel, Watt W. Webb†

Tryptophan and serotonin were imaged with infrared illumination by three-photon excitation (3PE) of their native ultraviolet (UV) fluorescence. This technique, established by 3PE cross section measurements of tryptophan and the monoamines serotonin and dopamine, circumvents the limitations imposed by photodamage, scattering, and indiscriminate background encountered in other UV microscopies. Three-dimensionally resolved images are presented along with measurements of the serotonin concentration (~50 mM) and content (up to ~5 × 10^8 molecules) of individual secretory granules.

Neurotransmitter granules have typically been studied either with various imaging techniques (*1*, *2*) that do not directly detect the granular content, or with chemical or electrical assays (*3*, *4*) that identify the granule contents but can probe only the extracellular medium. Thus, it has not been possible to determine neurotransmitter concentration or total neurotransmitter content of individual granules in intact cells. As a solution, we have excited the native UV fluorescence of these molecules by simultaneous absorption of three infrared photons, which accesses shorter wavelength UV transitions in living cells than conventional or two-photon microscopy (*5*).

When subjected to a high-intensity irradiation at wavelength λ, a molecule that ordinarily absorbs at λ/3 may exhibit fluorescence at ≳λ/3 by a three-photon absorption mechanism (*6*). The average fluorescence photon count rate F measured from three-photon excitation depends on the three-photon molecular absorption cross section σ_3 [unit: $(\text{length})^6\ (\text{time})^2\ (\text{photon})^{-2}$], the instantaneous intensity I, the fluorescence quantum efficiency Q, the detection efficiency K, the wavelength λ, and the concentration C (number of molecules per unit volume). Analogous with two-photon excitation (*7*), F is determined by the product of I^3 and C, integrated over space (r) and time (t'):

$$F = KQ\sigma_3[(1/\Delta t)\int_0^{\Delta t}\int_0^{\infty} I^3(\mathbf{r},t')C(\mathbf{r},t')\,d\mathbf{r}\,dt'] \quad (1)$$

For excitation of a homogeneous dye solution with a focused and pulsed laser beam with a gaussian temporal and spatial profile, the integral yields (SI units)

School of Applied and Engineering Physics, Cornell University, Ithaca, NY 14853, USA.

All authors contributed equally to this work.
*Present address: Department of Chemistry and Biochemistry, University of Texas, Austin, TX 78712, USA.
†To whom correspondence should be addressed.